



Polarization deconvolution and geophysical retrieval from a dual-pol, cross-track scanning microwave radiometer (AMPR) during OLYMPEX/RADEX

Sayak Biswas¹

Timothy Lang²

David Duncan³

Christian Kummerow³



¹*Universities Space Research Association*

²*NASA Marshall Space Flight Center*

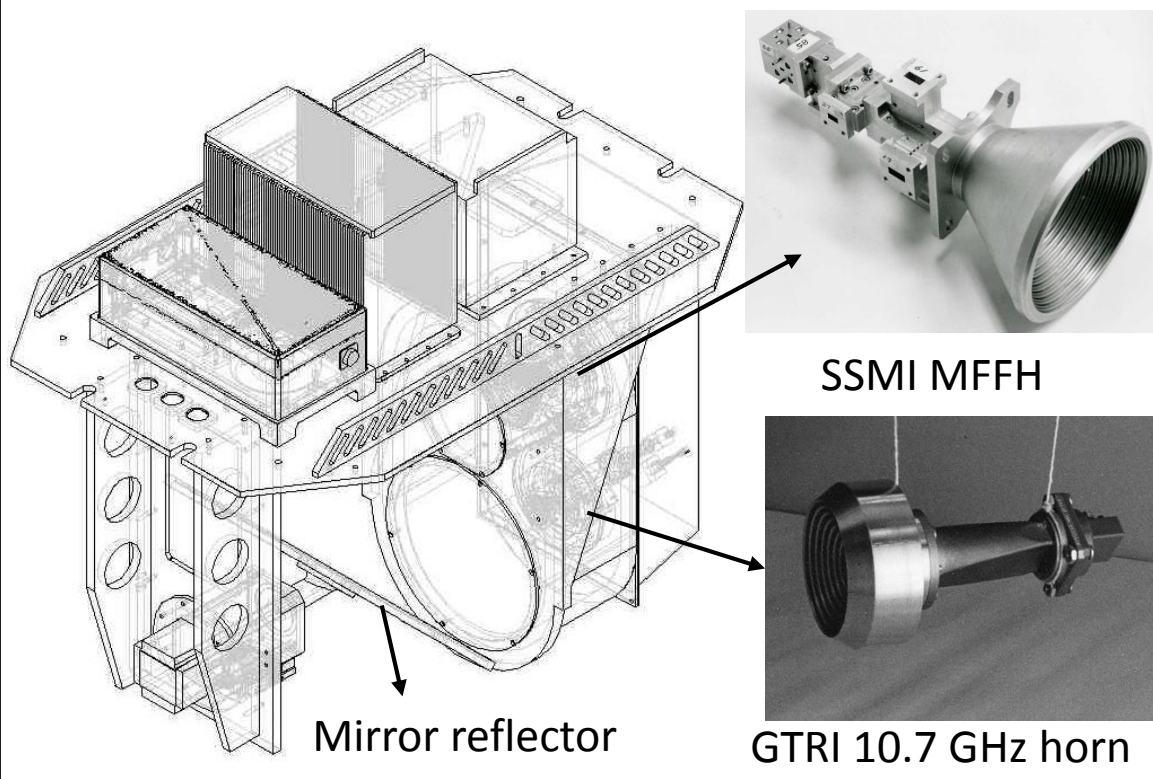
³*Colorado State University*



Outline

- Advance Microwave Precipitation Radiometer (AMPR) Instrument
- Polarization Mixing & Deconvolution
- Biases & Correction
- Retrieval
- Results

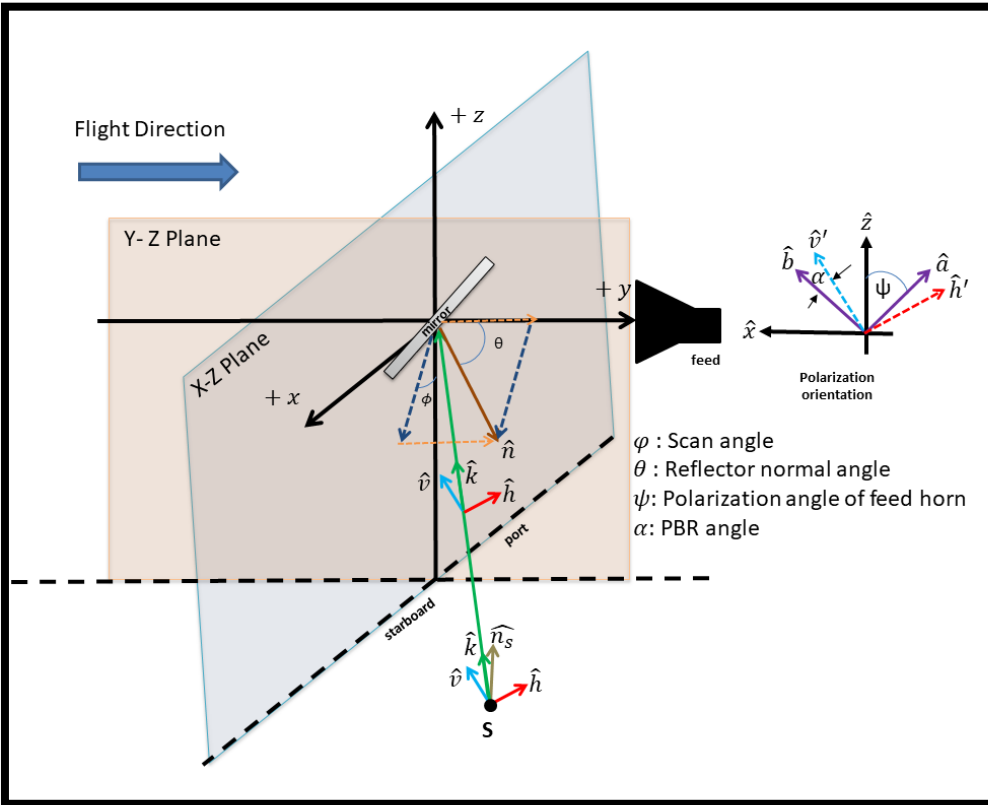
AMPR Instrument



Channel Center Frequency	85.5GHz	37.1GHz	19.35GHz	10.7GHz
Polarization	A/B	A/B	A/B	A/B
Pre Detection Bandwidth (MHz)	1400	900	240	100
Integration Time (ms)	50	50	50	50
Horn Type	SSM/I	SSM/I	SSM/I	GTRI
Lens Diameter (inches)	5.3	5.3	5.3	9.7
Beam width (degrees)	1.8	4.2	8.0	8.0
Footprint (km) [@20 km ER-2 alt. 500kts]	0.64	1.48	2.78	2.78

- Cross-track scanning microwave radiometer
- Feed horn polarization basis (A/B) rotates with respect to the scene polarization basis (V/H) as a function of scan angle.

Geometry of Polarization Basis Rotation



$$\begin{bmatrix} T_{F,B} \\ T_{F,A} \\ T_{F,U} \\ T_{F,V} \end{bmatrix} = \begin{bmatrix} \cos^2 \alpha & \sin^2 \alpha & \frac{1}{2} \sin 2\alpha & 0 \\ \sin^2 \alpha & \cos^2 \alpha & -\frac{1}{2} \sin 2\alpha & 0 \\ -\sin 2\alpha & \sin 2\alpha & \cos 2\alpha & 0 \\ 0 & 0 & 0 & 1 \end{bmatrix} \begin{bmatrix} T_{E,v} \\ T_{E,h} \\ T_{E,U} \\ T_{E,V} \end{bmatrix}$$

$$\alpha = \tan^{-1} \left[\frac{\{\cos 2\theta \sin \psi + 2 \sin^2 \theta \sin \phi \sin(\phi - \psi)\}}{\{\cos 2\theta \sin \psi + 2 \sin^2 \theta \sin \phi \cos(\phi - \psi)\}} \right]$$

In AMPR, $\theta = 45^\circ$.

Therefore, $\alpha = \phi - \psi$

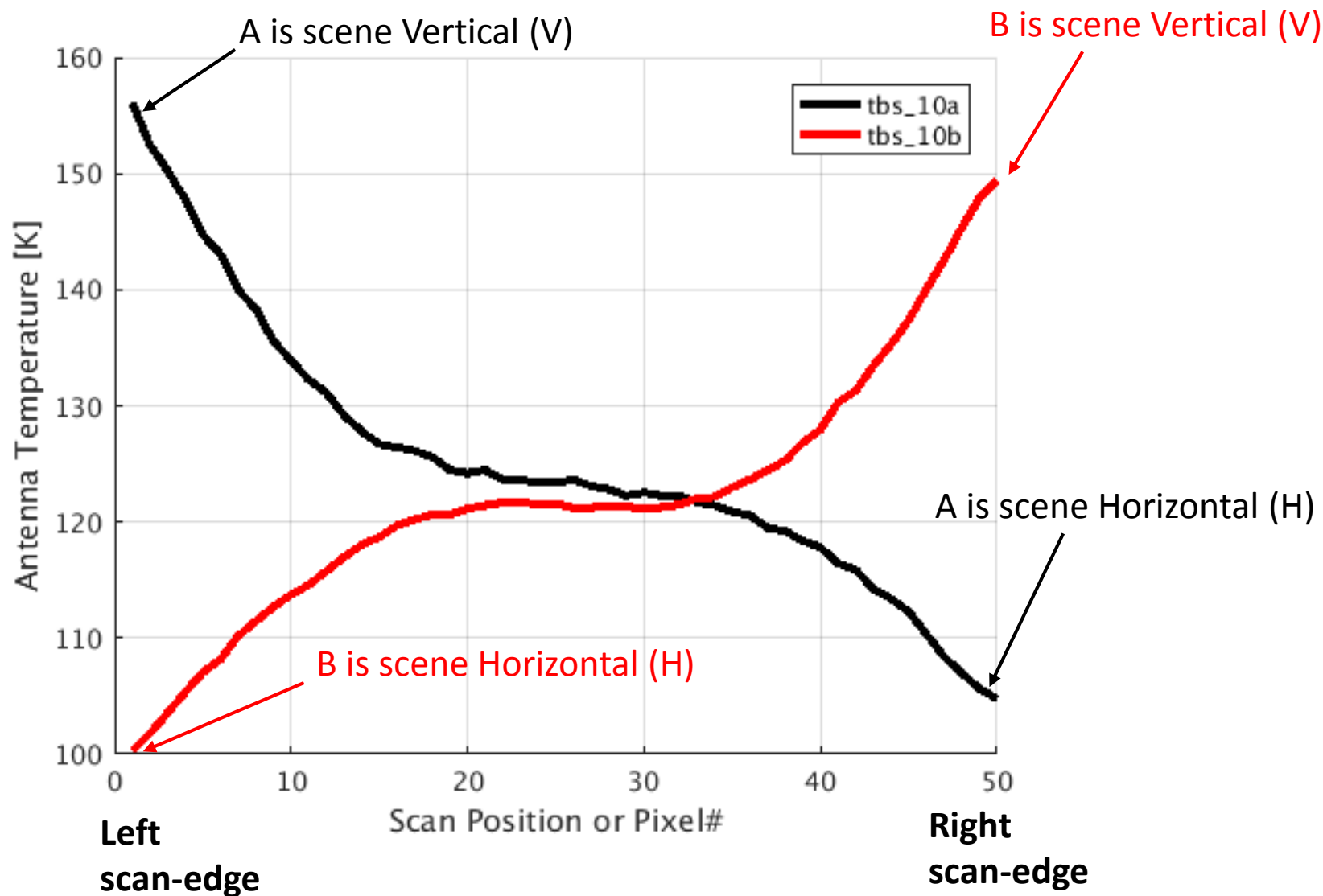
Since, the modified 3rd (T_U) and 4th (T_V) stokes brightness temperatures are not measured, the simplified transform is:

$$\begin{bmatrix} T_{F,B} \\ T_{F,A} \end{bmatrix} = \begin{bmatrix} \cos^2 \alpha & \sin^2 \alpha \\ \sin^2 \alpha & \cos^2 \alpha \end{bmatrix} \begin{bmatrix} T_{E,v} \\ T_{E,h} \end{bmatrix}$$

Where,

$$\alpha = \phi - 45^0$$

Geometry of Polarization Basis Rotation



Observed Bias in recovered V & H –pol Brightness Temperature (Tb)

- The relationship between Tb measured in instrument polarization basis (A,B) and the scene polarization basis (V,H) is given by,

$$\begin{bmatrix} T_V \\ T_H \end{bmatrix} = \begin{bmatrix} \sin^2(45 - \phi) & \cos^2(45 - \phi) \\ \cos^2(45 - \phi) & \sin^2(45 - \phi) \end{bmatrix} \begin{bmatrix} T_A \\ T_B \end{bmatrix} \quad (1)$$

- Equation (1) is used to create observed V,H –pol Tb data from AMPR measurements.
- Tb Bias = Tb (Observed) – Tb (Simulated)
- GDAS profiles and SST information was used to simulate V,H –pol TB for several OLYMPEX flights with data over ocean.

Bias sources

- The Tb bias for any AMPR polarization channel (A or B) is defined as,

$$\Delta T_b = T_b^{\text{OBSERVED}} - T_b^{\text{SIMULATED}}$$

where,

$$T_b^{\text{SIMULATED}} = (1-\eta) * [A(\theta, \psi, \phi) * T_b^V + B(\theta, \psi, \phi) * T_b^H] \\ + \eta * [B(\theta, \psi, \phi) * T_b^V + A(\theta, \psi, \phi) * T_b^H] \quad (2)$$

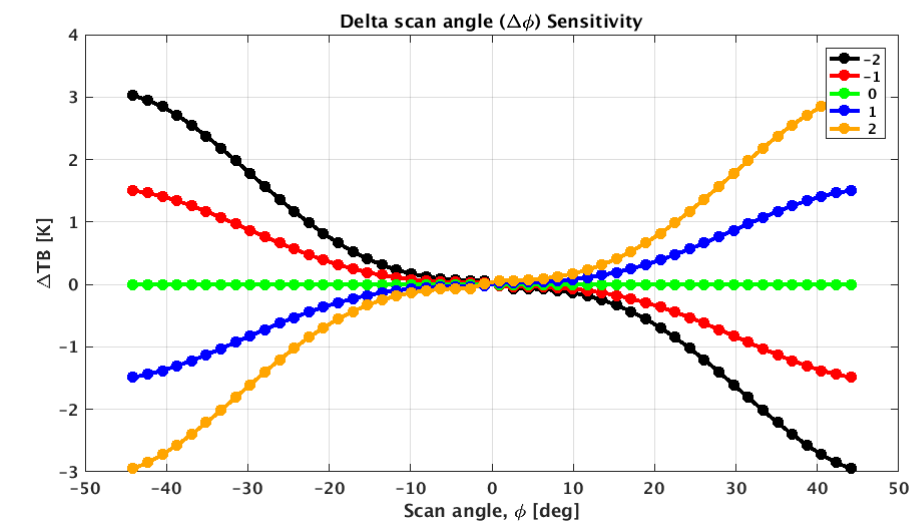
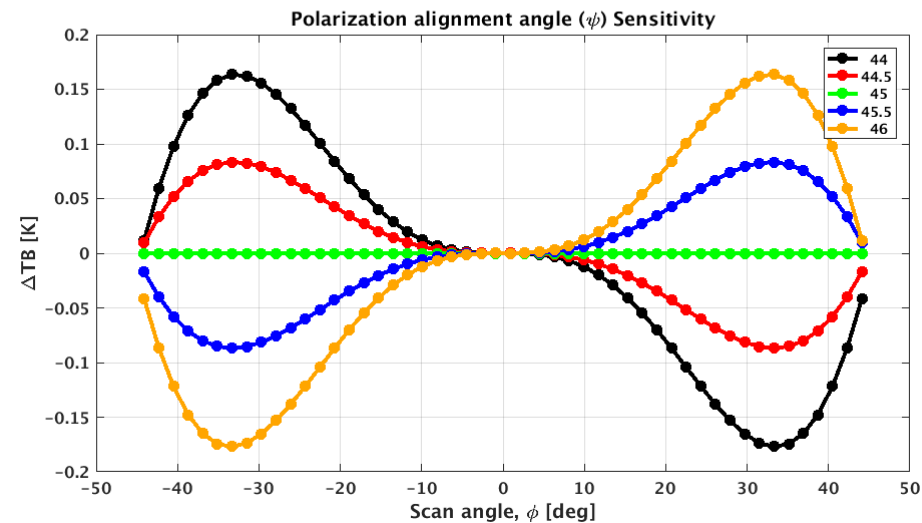
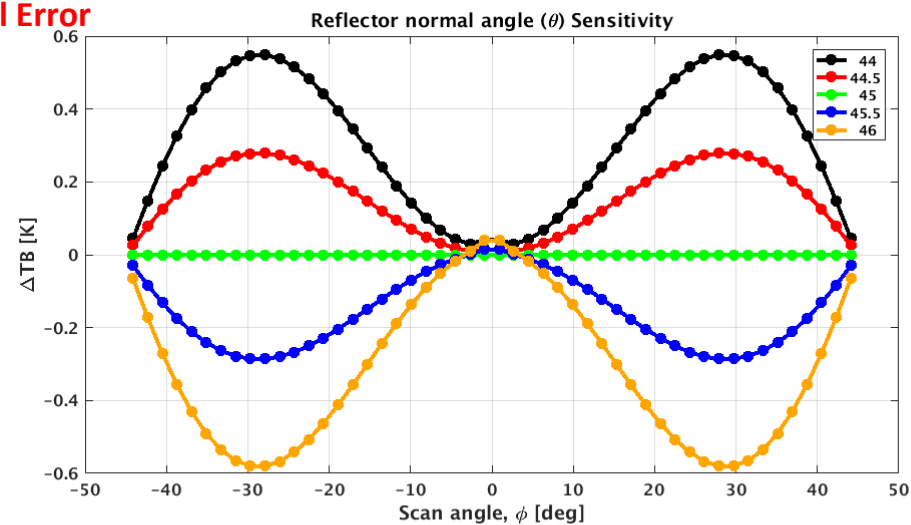
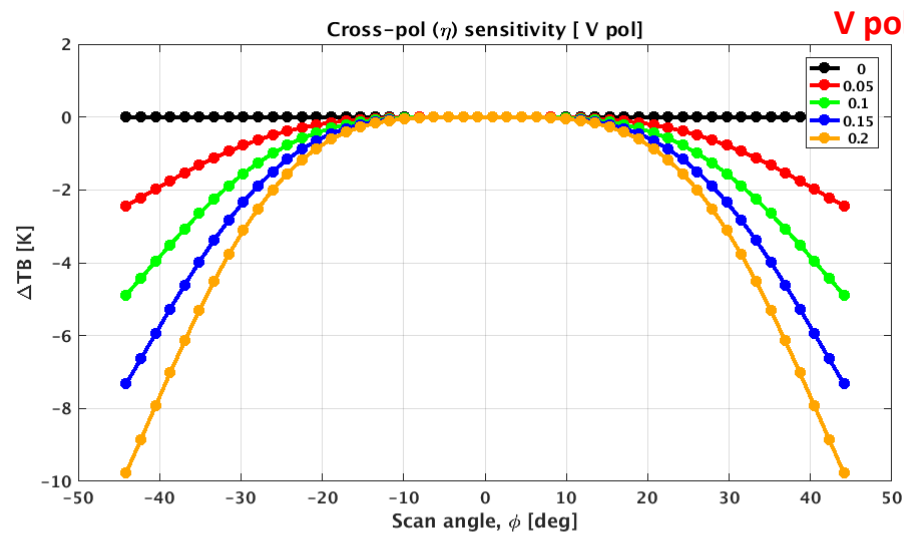
η = cross polarization fraction

A,B = polarization mixing weights (function of geometry)

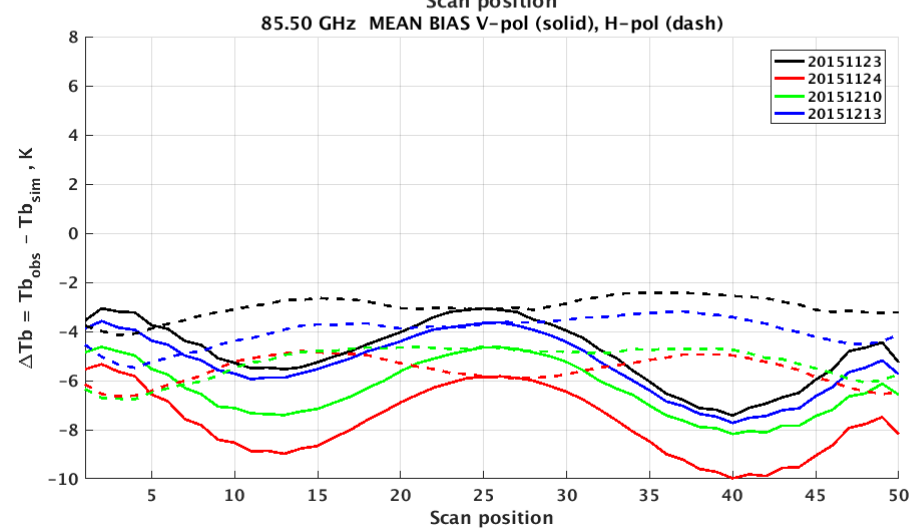
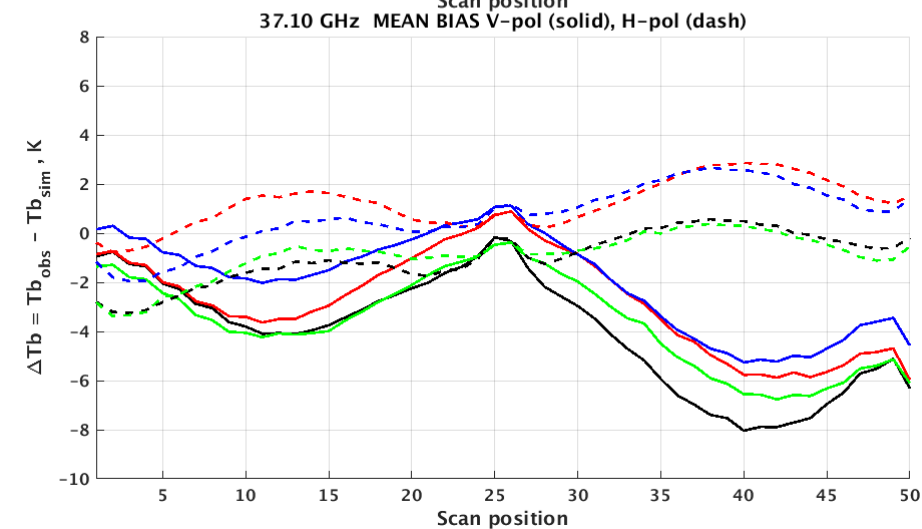
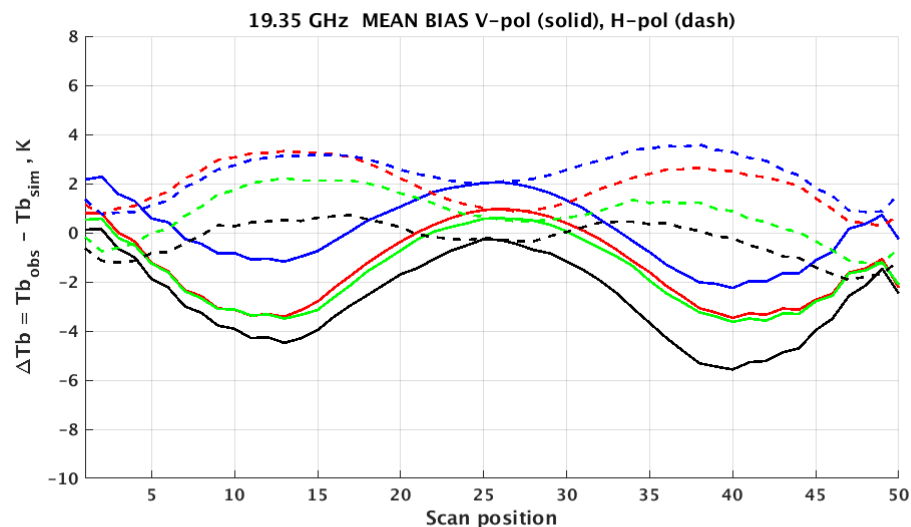
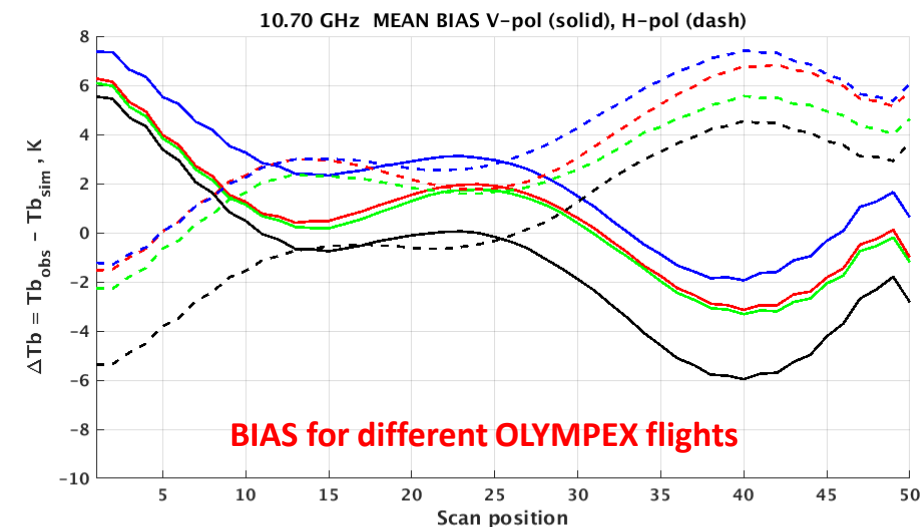
θ, ψ, ϕ = reflector normal angle, polarization alignment angle, sensor scan angle

- Any deviation of the following parameters from the nominal values will result in a bias:
 η, θ, ψ, ϕ
- A simulator is developed to analyze the bias sensitivity to any of the above parameters

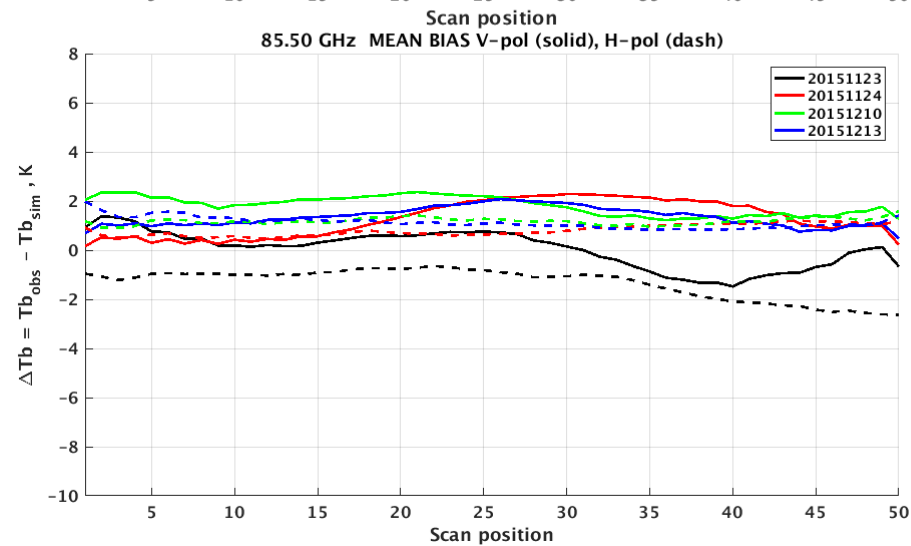
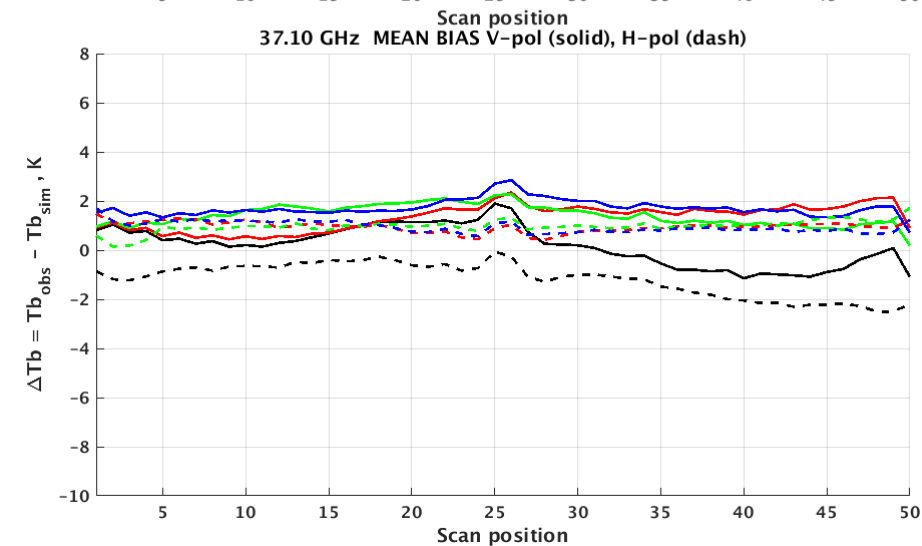
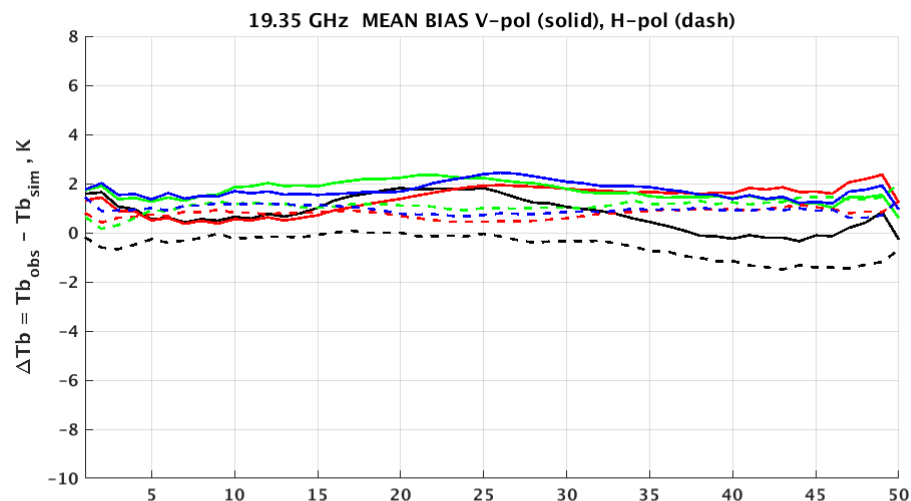
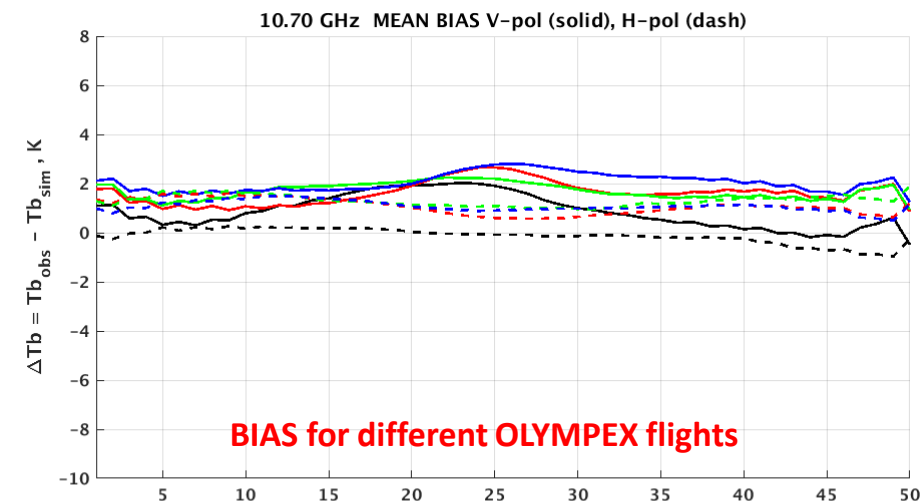
V-pol Bias Due to Angle Error



V & H-pol Tb Bias



V & H –pol Tb Bias – AFTER CORRECTION



Multi-Linear Regression Model(s)

- Model for Columnar Water Vapor (V in mm):

$$V \text{ (mm)} = a_0 + a_1 * T_{B10v} + a_2 * T_{B10h} + a_3 * \ln(290 - T_{B19v}) + a_4 * \ln(290 - T_{B19h}) + a_5 * \ln(290 - T_{B37v}) + a_6 * \ln(290 - T_{B37h})$$

- Model for Columnar Cloud Liquid Water (L in mm):

$$L \text{ (mm)} = a_0 + a_1 * \ln(290 - T_{B19v}) + a_2 * \ln(290 - T_{B19h}) + a_3 * \ln(295 - T_{B85v}) + a_4 * \ln(295 - T_{B85h})$$

- Model for Surface Wind Speed (WS in m/s):

$$WS \text{ (m/s)} = a_0 + a_1 * T_{B10v} + a_2 * T_{B10h} + a_3 * \ln(290 - T_{B19v}) + a_4 * \ln(290 - T_{B19h}) + a_5 * T_{B10v}^2 + a_6 * T_{B10h}^2 + a_7 * T_{B10v} * T_{B10h} + a_8 * SST$$

Where, $T_{Bnv,h}$ = Measured T_B for n GHz v,h-polarization channels

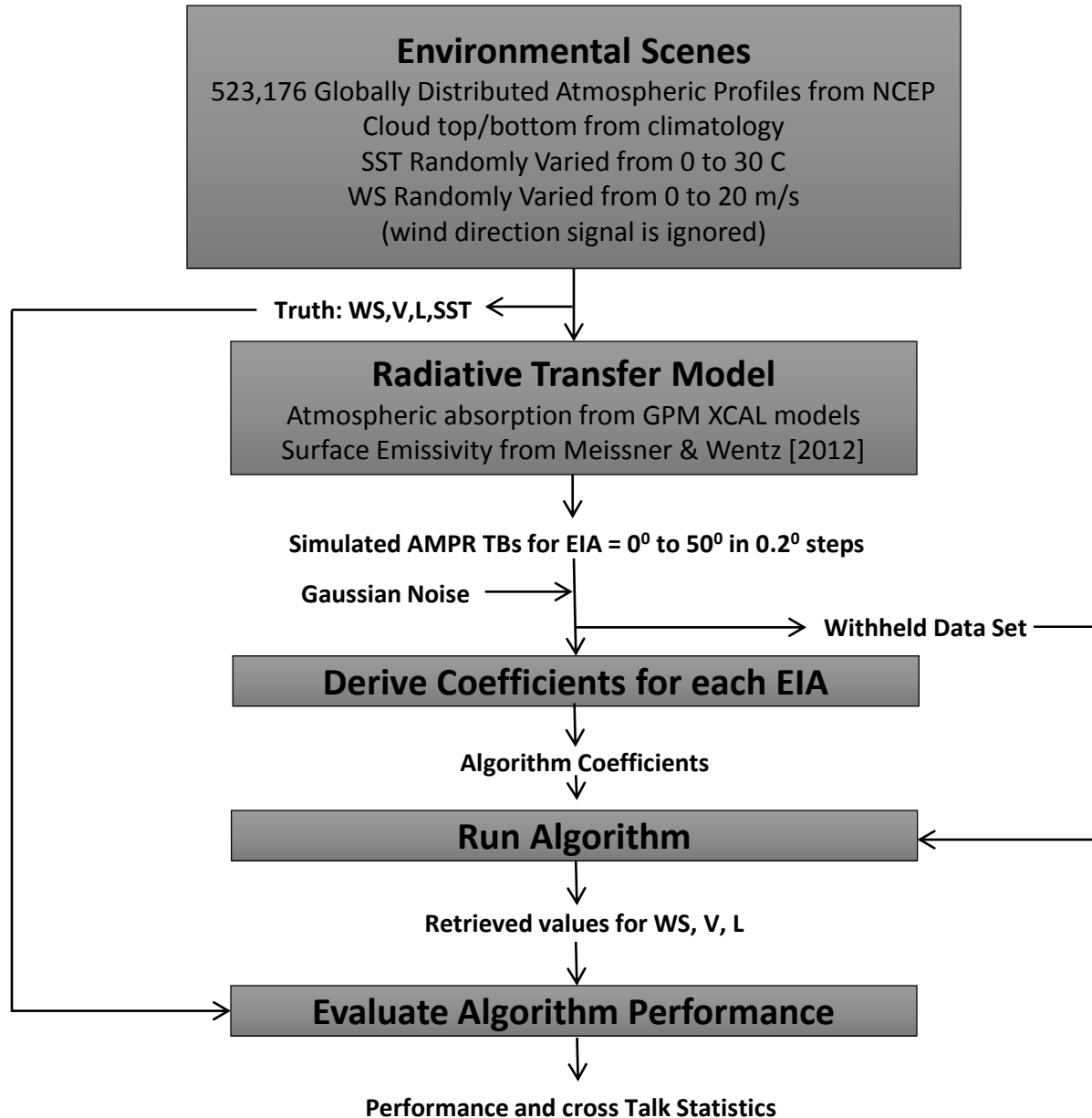
SST = Sea Surface Temperature in kelvin (a priori value needed)

a_n coefficients are polynomial functions of the incidence angle*

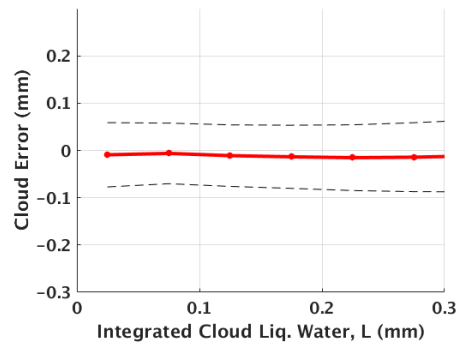
The WS retrieval is further improved by generating 'a' coefficients for different range of wind speeds, e.g. $WS \leq 3$, $3 < WS \leq 7$, $7 < WS \leq 12$ & $WS > 12$.

(*AMPR is a cross-track scanner and the observation incidence angle varies between 0° to 45°)

Coefficient Derivation & Testing

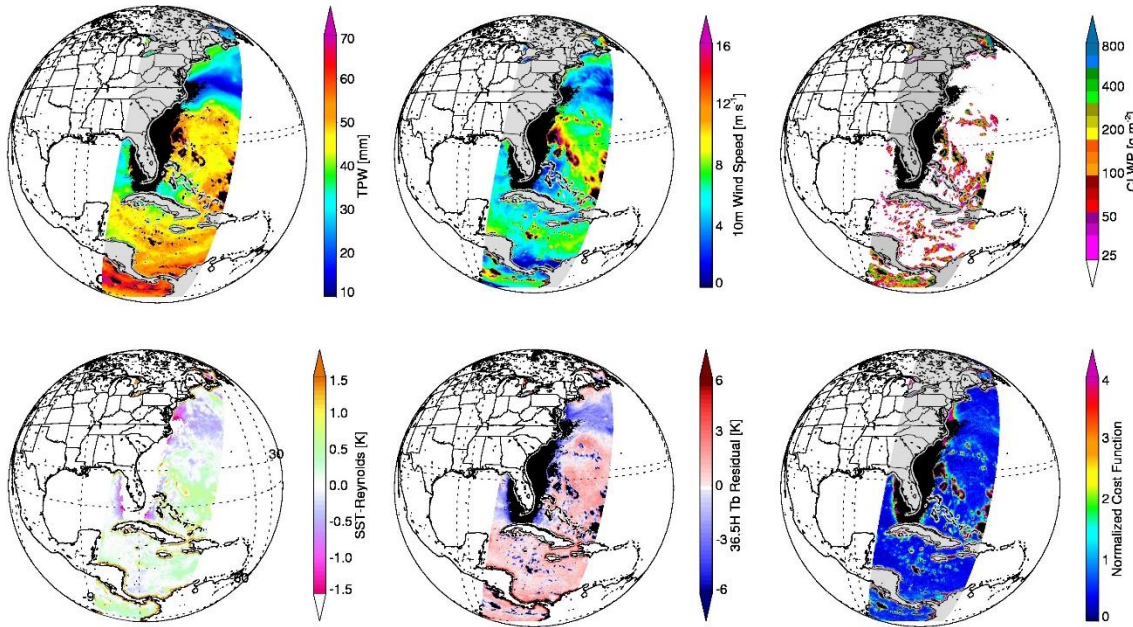


Errors are averaged over all EIA between 0 to 50 deg

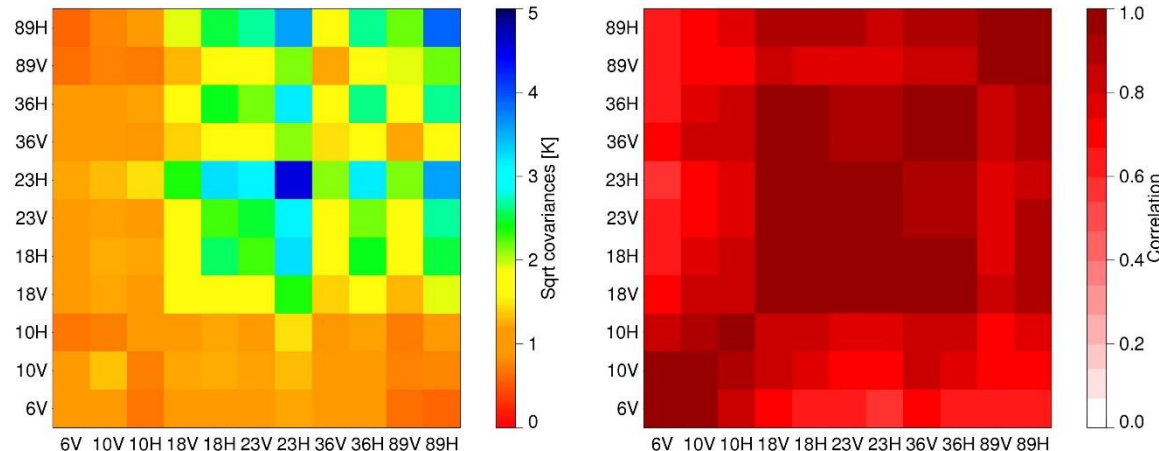


EIA average RMS Retrieval Error	
WS (m/s)	0.9
V (mm)	1.85
L (mm)	0.11

CSU 1DVAR



- Optimal estimation retrieval for microwave imagers over ocean
- Simultaneously solve for wind speed, SST, liquid water path, and water vapor profile
- CRTM with FASTEM6 in forward model
- Water vapor profile decomposed into principal components
- Novel observation error covariance matrix accounts for co-varying forward model errors
- Applicable to any imager platform due to physical forward model
- See Duncan and Kummerow (2016) for additional details

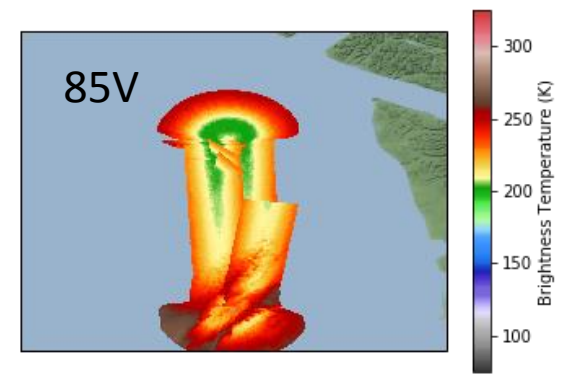
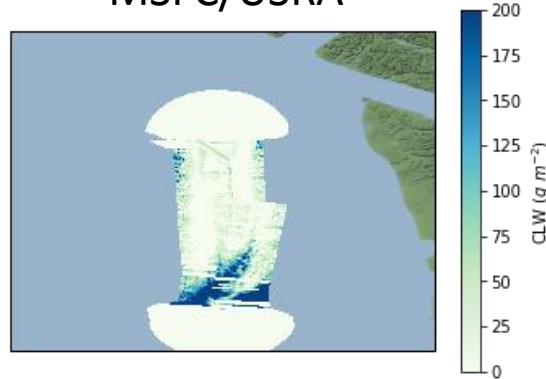
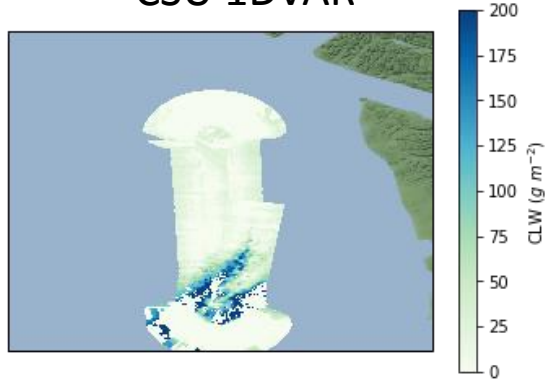


11/24/15 2000-2038 UTC

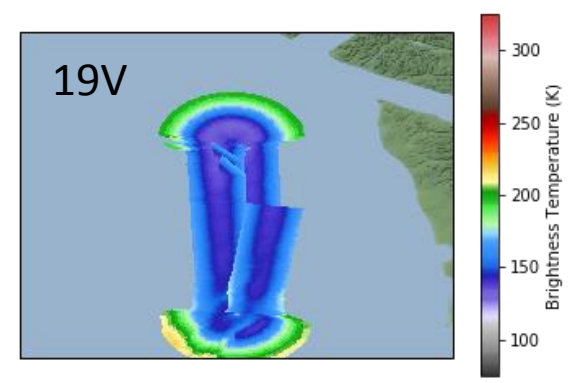
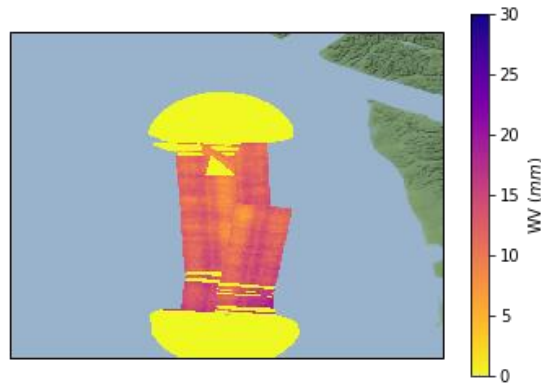
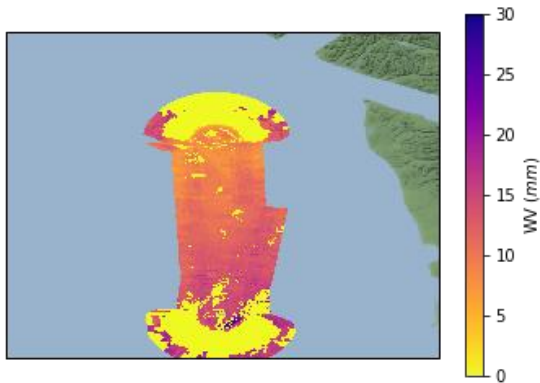
CSU 1DVAR

MSFC/USRA

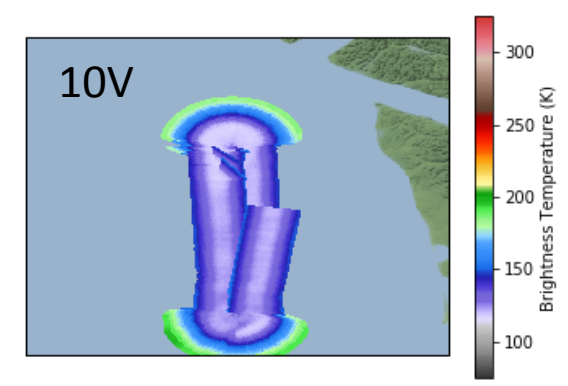
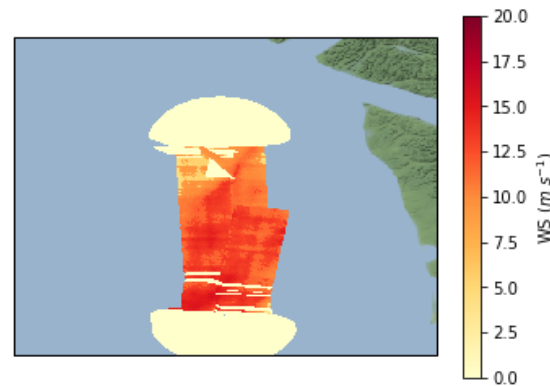
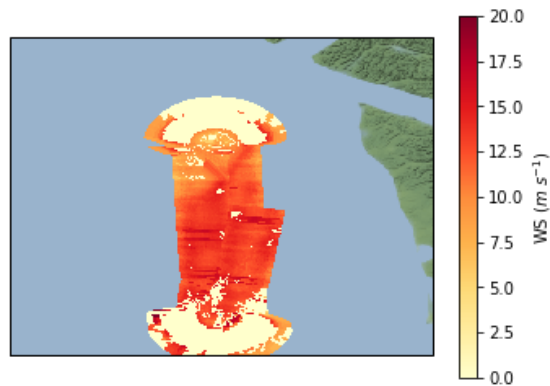
CLW



WV

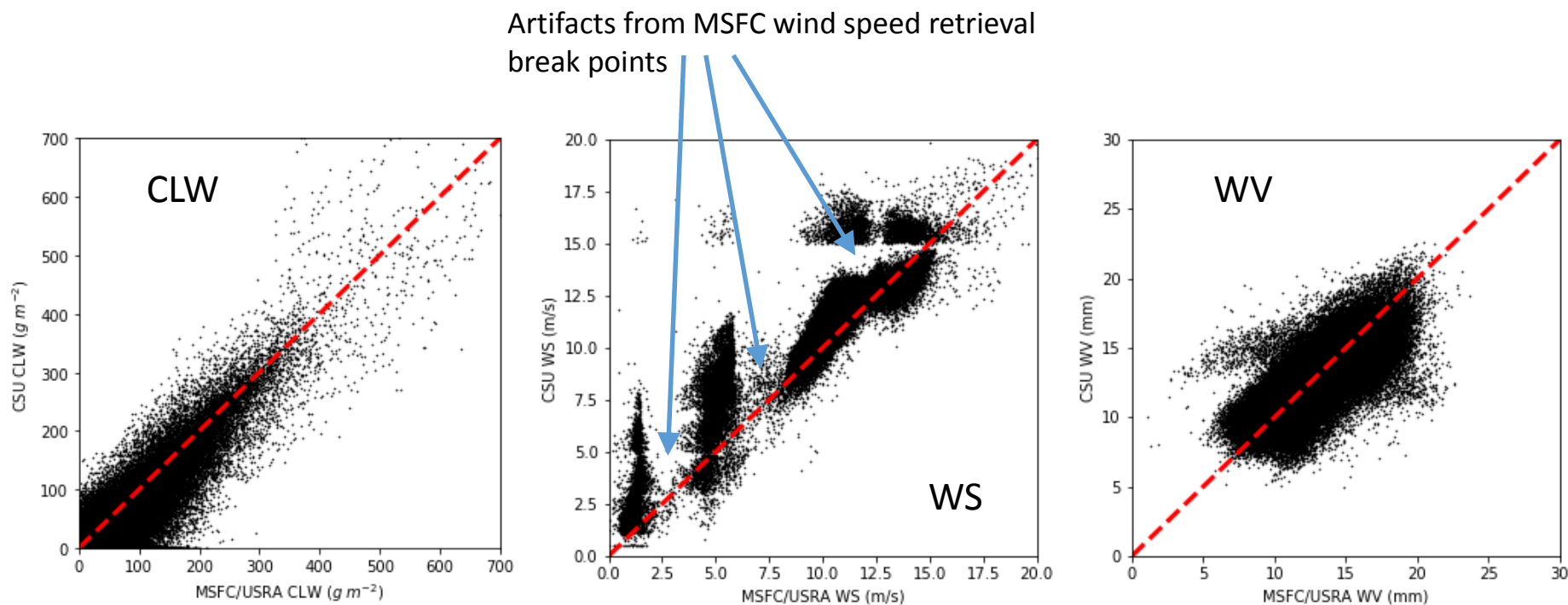


WS



Comparison between CSU 1DVAR Algorithm and MSFC/USRA Algorithm for 11/24/2015

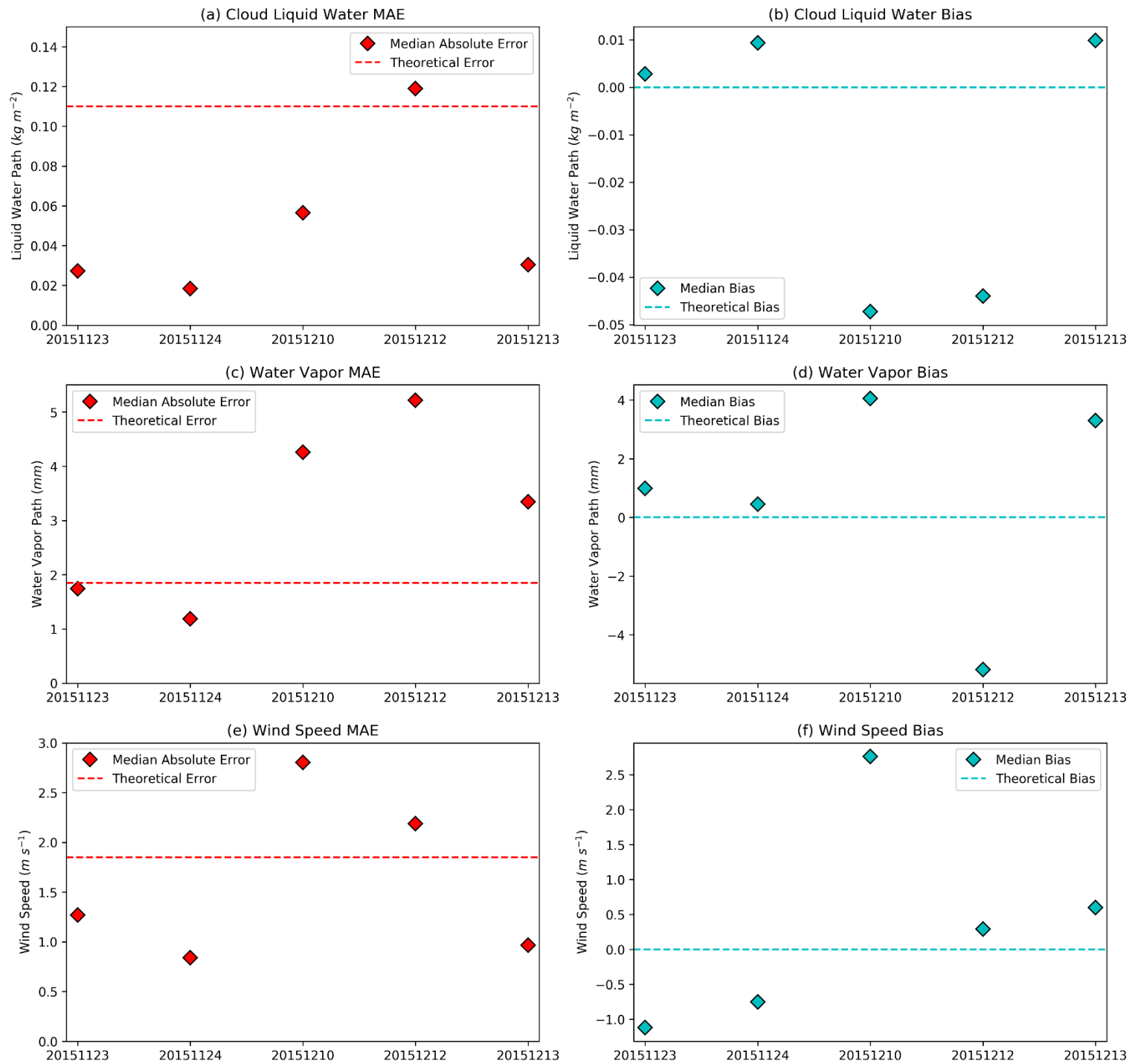
- CLW good agreement overall
- WV and WS impacted by artifacts resulting from MSFC algorithm
- MSFC retrieves even in possibly raining scenarios
- CSU masks potential precip-impacted regions, but sometimes mask fails leading to highly erroneous retrievals



MSFC vs. CSU Algorithms

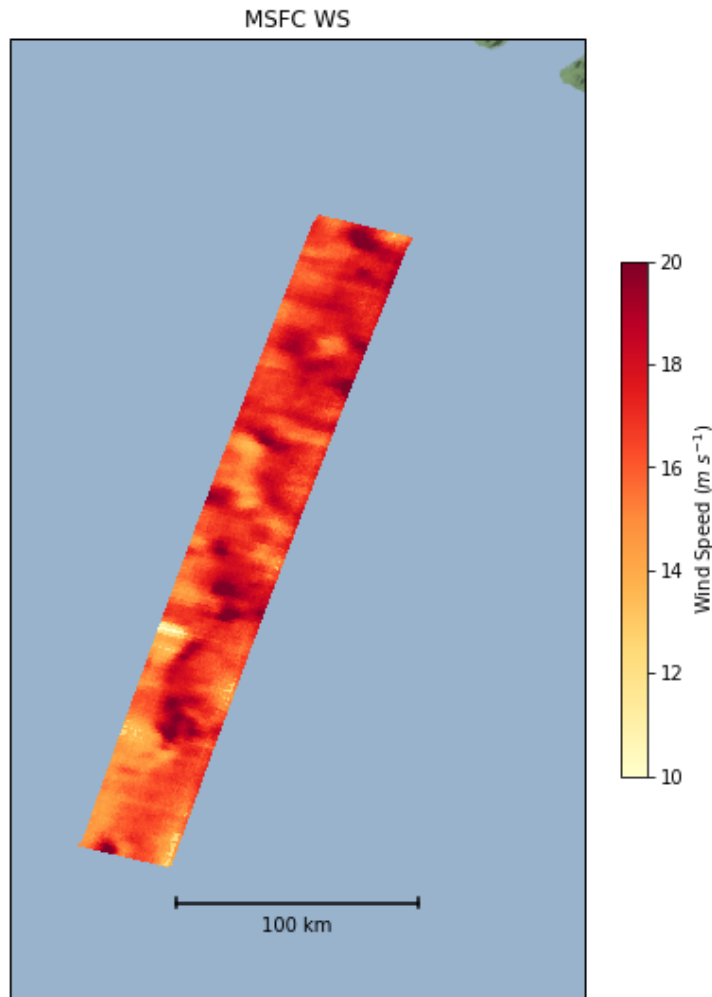
Five different case days

11/23, 24
12/10, 12, 13

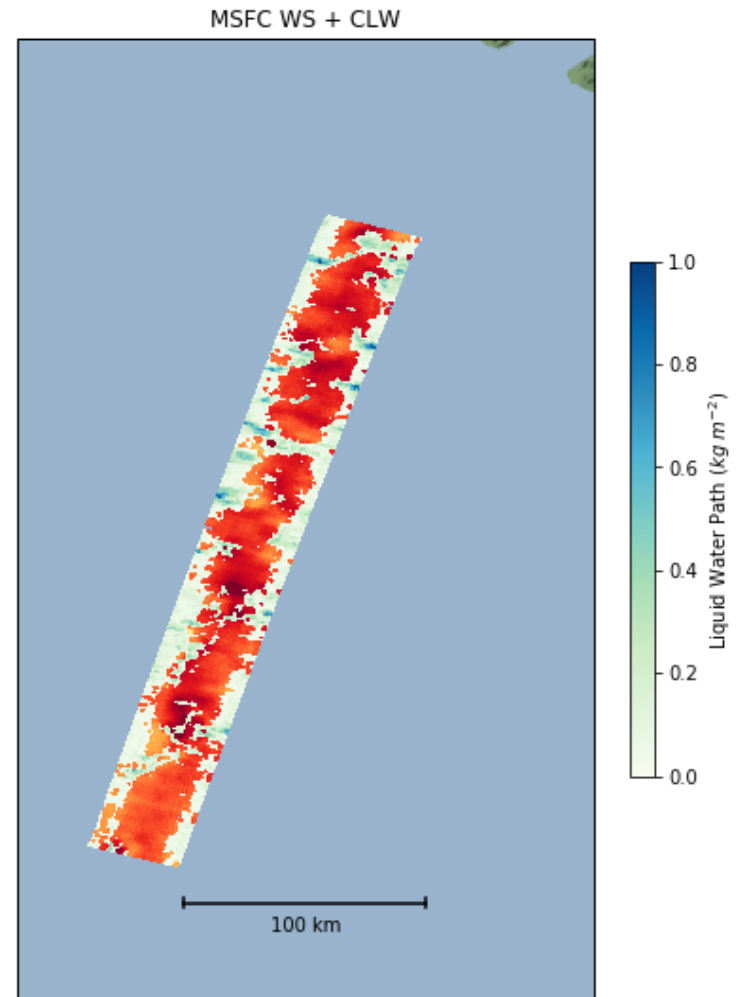


12/13, 1916-1947 UTC

Small-scale variability in WS suggests post-frontal convection influencing surface winds



“Lumpiness”



Wind speed masked for $\text{CLW} > 0.01 \text{ kg m}^{-2}$

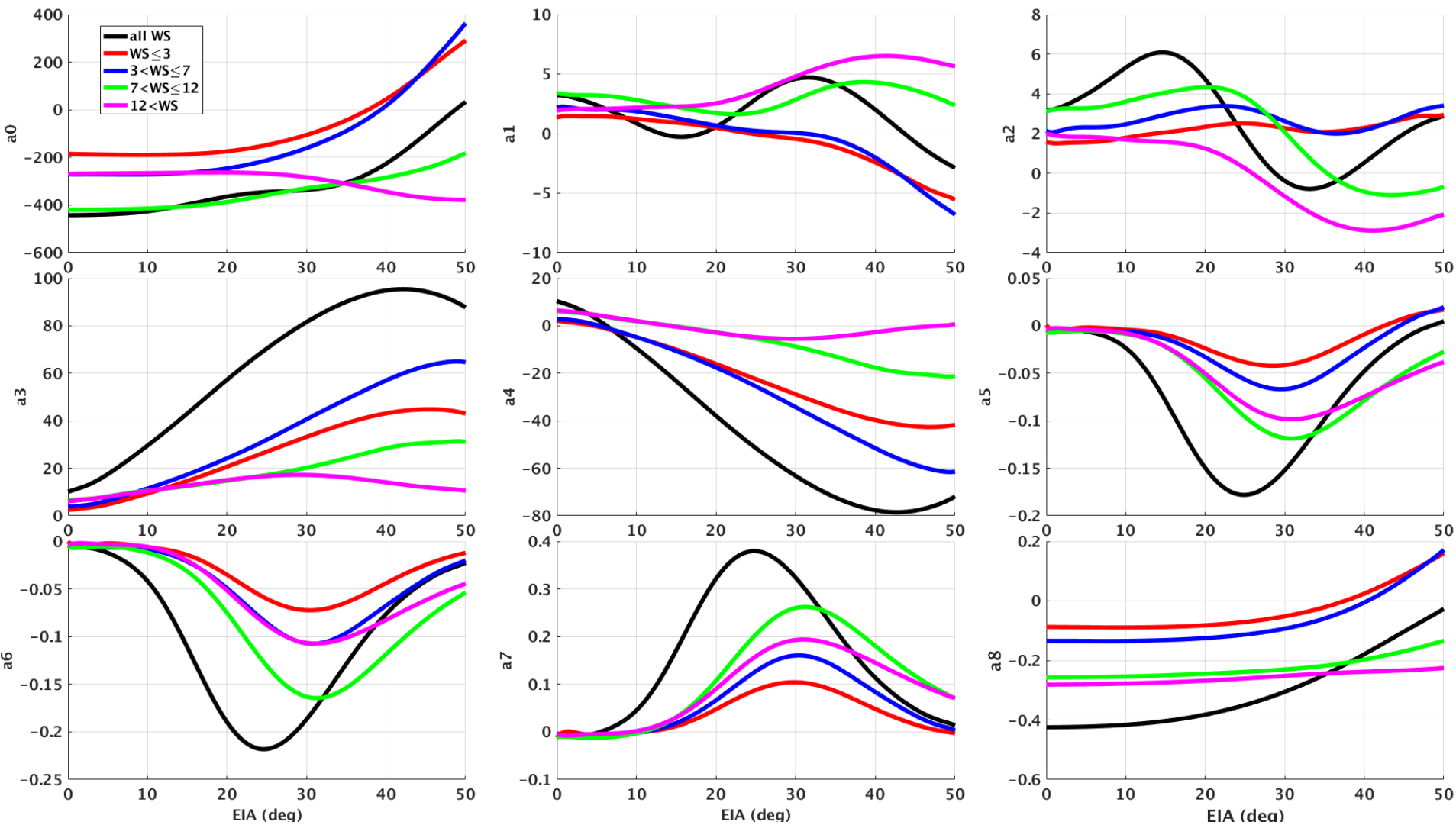
Conclusions

- Significant improvements have been made to AMPR brightness temperature measurements, enabling deconvolution to V and H polarizations and the retrieval of physically realistic values for CLW, WV, and WS.
- Some artifacts still remain, due to instrument uncertainties as well as algorithm limitations – Improvement efforts continue
- MSFC algorithm capable of detecting apparent small-scale variability in convectively driven winds outside post-frontal cells on 12/13

Acknowledgement:

BACKUP

WS regression coefficients

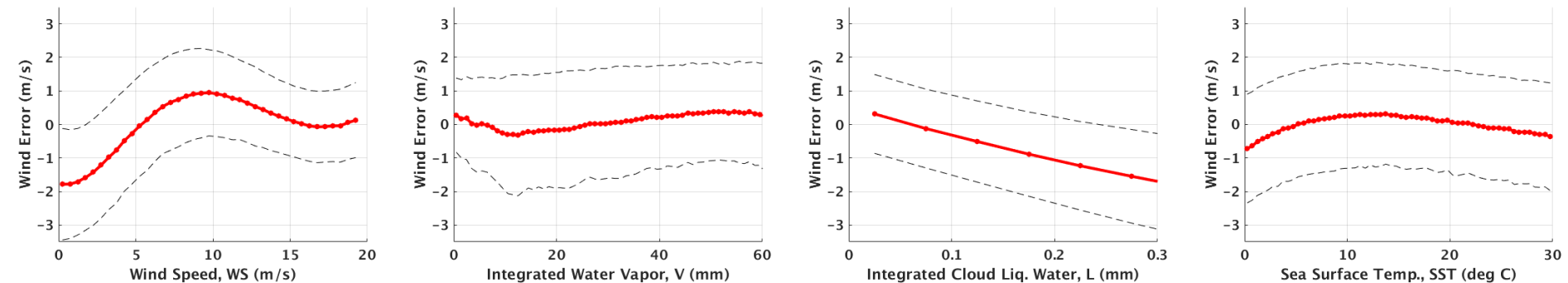


Two step retrieval:

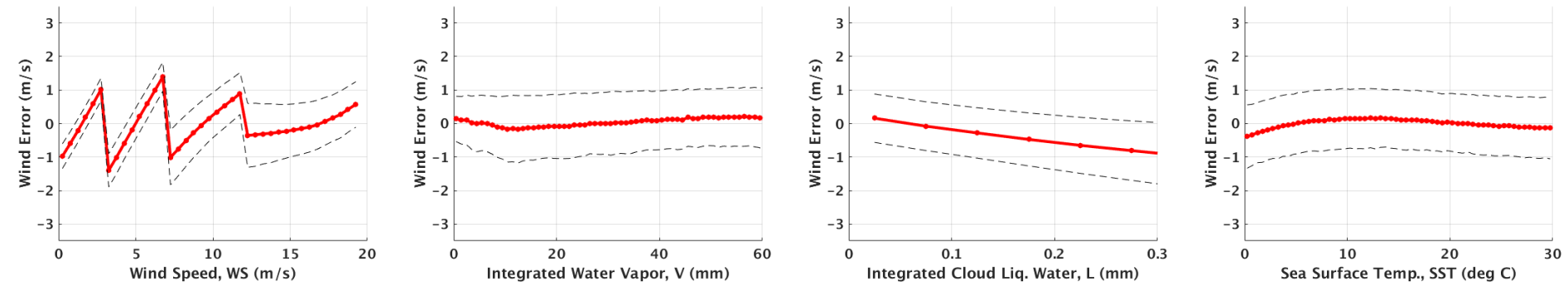
1. “all WS” coefficients are used for the first retrieval.
2. Depending on the retrieved WS value of “all WS” algorithm, corresponding set of coefficients are chosen for a second and final retrieval.

Performance Comparison of Two step WS algorithm and One step algorithm

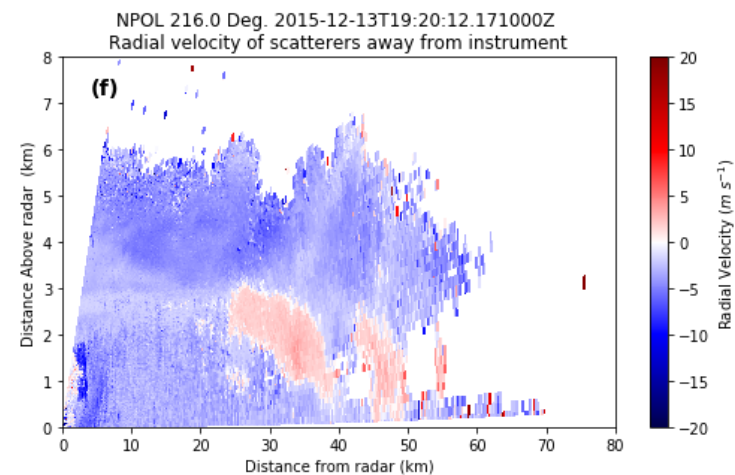
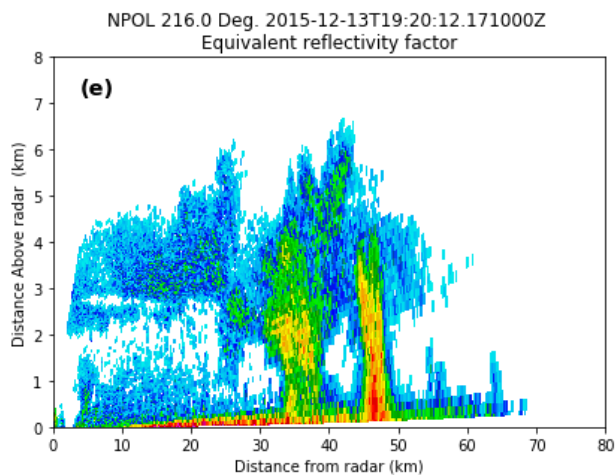
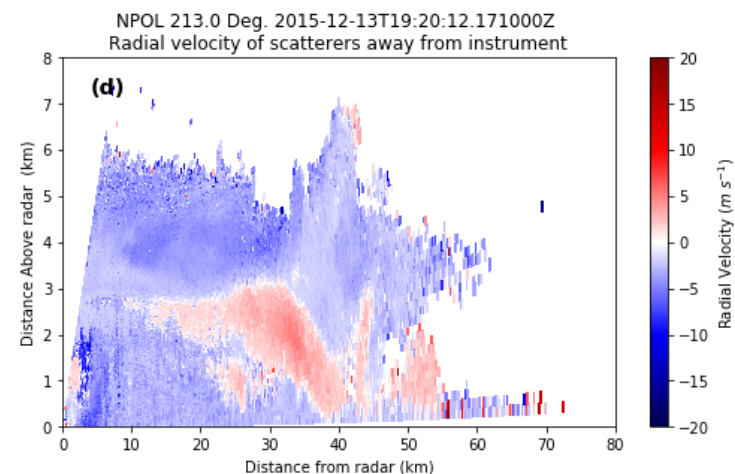
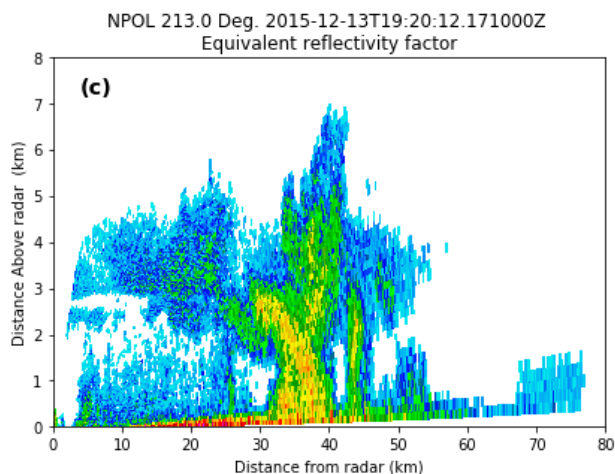
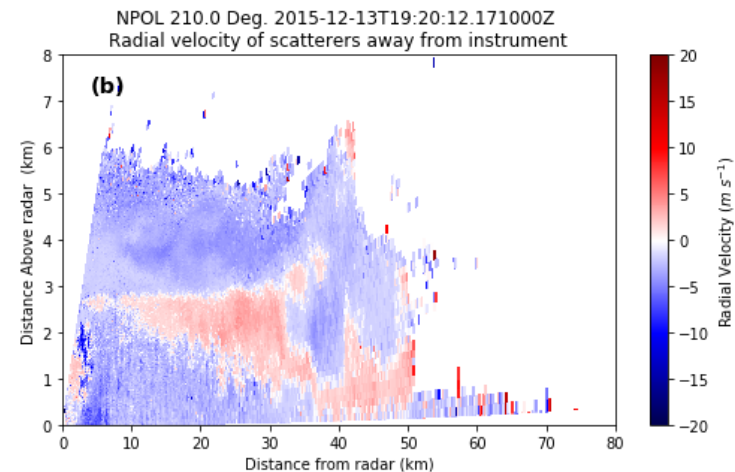
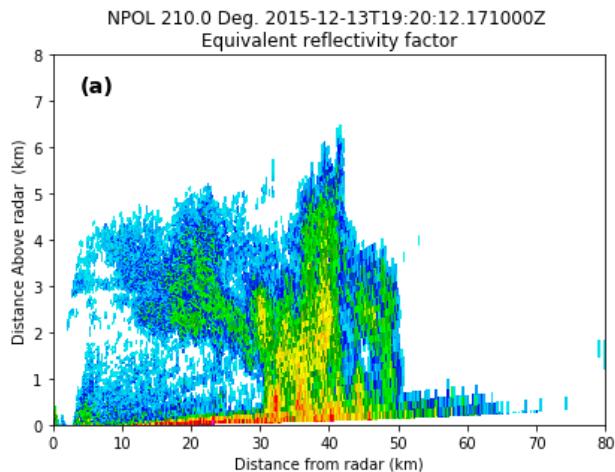
One Step Algorithm Error & Error correlation

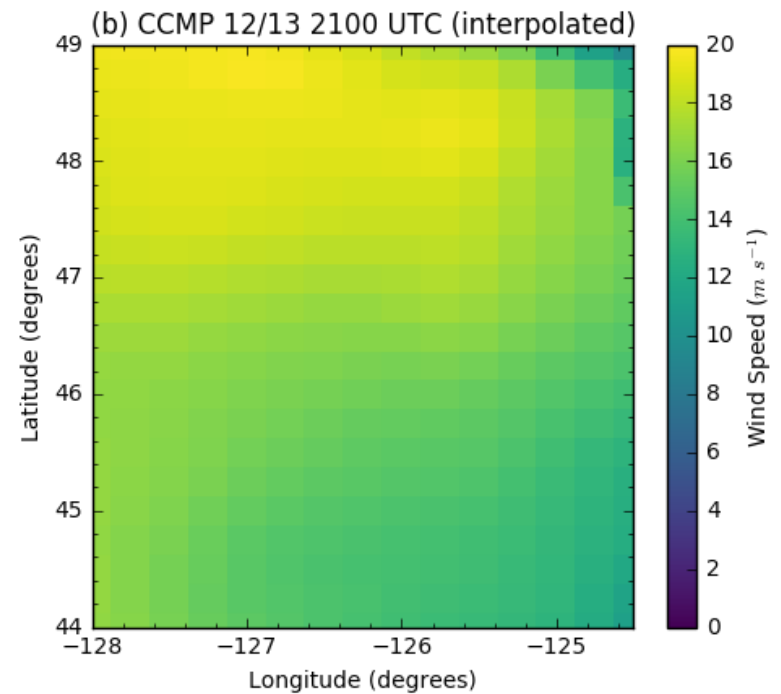
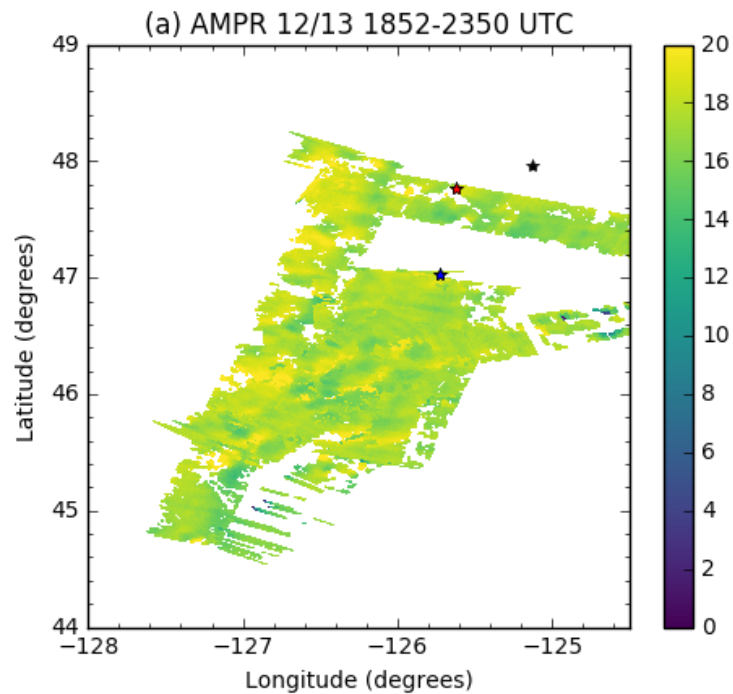


Two Step Algorithm Error & Error correlation



'red' solid line is the mean error (averaged over all incidence angles).
Dashed line show the ± 1 std. deviation of the error about the mean value
Two step algorithm performs better as expected.





12/13 dropsonde comparison

Dropsondes > 1 h from AMPR;
however, closest one (red star) within
 $1.2 m s^{-1}$

